Flexpart v10.1 simulation of source contributions to Arctic black carbon

Chunmao Zhu[1], Yugo Kanaya[1,2], Masayuki Takigawa[1,2], Kohei Ikeda[3], Hiroshi Tanimoto[3], Fumikazu Taketani[1,2], Takuma Miyakawa[1,2], Hideki Kobayashi[1,2], Ignacio Pisso[4]

[1]Research Institute for Global Change, Japan Agency for Marine–Earth Science and Technology (JAMSTEC), Yokohama 2360001, Japan

[2]Institute of Arctic Climate and Environmental Research, Japan Agency for Marine–Earth Science and Technology, Yokohama 2360001, Japan

[3]National Institute for Environmental Studies, Tsukuba 305-8506, Japan

[4]NILU – Norwegian Institute for Air Research, Kjeller 2027, Norway

Correspondence to Chunmao Zhu (chmzhu@jamstec.go.jp)

Abstract

The Arctic environment is undergoing rapid changes such as faster warming than the global average and exceptional melting of glaciers in Greenland. Black carbon (BC) particles, which are a short-lived climate pollutant, are one cause of Arctic warming and glacier melting. However, the sources of BC particles are still uncertain. We simulated the potential emission sensitivity of atmospheric BC present over the Arctic (north of 66° N) using the Flexpart Lagrangian transport model (version 10.1). This version includes a new aerosol wet removal scheme, which better represents particle-scavenging processes than older versions did. Arctic BC at the surface (0–500 m) and high altitudes (4750–5250 m) is sensitive to emissions in high latitude (north of 60° N) and mid-latitude (30–60° N) regions, respectively. Geospatial sources of Arctic BC were quantified, with a focus on emissions from anthropogenic activities (including domestic biofuel burning) and open biomass burning (including agricultural burning in the open field) in 2010. We found that anthropogenic sources contributed 82 % and 83 % of annual Arctic BC at the surface and high altitudes, respectively. Arctic surface BC comes predominantly from anthropogenic emissions in Russia (56 %), with gas flaring from the Yamalo-Nenets Autonomous Okrug and Komi Republic being the main source (31 % of Arctic surface BC). These results highlight the need for regulations to control BC emissions from gas flaring to mitigate the rapid changes in the Arctic environment. In summer, combined open biomass burning in Siberia, Alaska, and Canada contributes 56–85 % (75 % on average) and 40–72 % (57 %) of Arctic BC at the surface and high altitudes, respectively. A large fraction (40 %) of BC in the Arctic at high altitudes comes from anthropogenic emissions in East Asia, which suggests that the rapidly growing economies of developing countries could have a non-negligible effect on the Arctic. To our knowledge, this is the first year-round evaluation of Arctic BC sources that has been

performed using the new wet deposition scheme in Flexpart. The study provides a scientific basis for actions to mitigate the rapidly changing Arctic environment.

1 Introduction

The Arctic region has experienced warming at a rate twice that of the global average in recent decades (Cohen et al., 2014). The Arctic cryosphere has been undergoing unprecedented changes since the mid-1800s (Trusel et al., 2018). Glacier cover in Greenland reached its historically lowest level in summer 2012 (Tilling et al., 2015). Evidence indicates that the emissions and transport of greenhouse gases and aerosols to the Arctic region are contributing to such warming and melting of snow and ice (Keegan et al., 2014; Najafi et al., 2015). Short-lived climate pollutants such as black carbon (BC) particles, tropospheric ozone, and methane greatly affect the Arctic climate (AMAP, 2015; Quinn et al., 2008).

BC particles are emitted during incomplete combustion of fossil fuels, biofuels, and biomass. BC warms the atmosphere by direct absorption of solar radiation. The deposition of BC on snow and ice surfaces accelerates their melting through decreasing albedo, which contributes to the rapid loss of glaciers. In the Arctic region, ground-based observations have indicated that BC shows clear seasonal variations, with elevated mass concentrations in winter and spring (the so-called Arctic haze) and low values in summer (Law and Stohl, 2007). Such seasonal variations are explained by increased transport from lower latitudes in the cold season and increased wet scavenging in the warm season (Shaw, 1995; Garrett et al., 2011; Shen et al., 2017).

The presence of BC particles in the Arctic is mainly attributed to emissions in high-latitude regions outside the Arctic, such as northern Europe and Russia (Stohl, 2006; Brock et al., 2011). This is partly caused by the polar dome (Stohl, 2006), which is formed because of the presence of constant potential temperature near the surface. The emissions in high-latitude regions are transported to the Arctic region and trapped in the dome, which increases the surface concentration. Recently, Schmale et al. (2018) suggested that local emissions from

within the Arctic are another important source, and these are expected to increase in the future.

Although numerous studies have been performed, results regarding regional contributions of BC sources in the Arctic are still inconclusive. For example, ground-based observations and Lagrangian transport model results reported by Winiger et al. (2016) showed that BC in Arctic Scandinavia is predominantly linked to emissions in Europe. Over the whole Arctic region (north of 66° N), Russia contributes 62 % to surface BC in terms of the annual mean (Ikeda et al., 2017). Gas flaring in Russia has been identified as a major (42 %) source of BC at the Arctic surface (Stohl et al., 2013). Xu et al. (2017) found that anthropogenic emissions from northern Asia contribute 40–45 % of Arctic surface BC in winter and spring. However, the results of some other studies have suggested that Russia, Europe, and South Asia each contribute 20–25 % of BC to the low-altitude springtime Arctic haze (Koch and Hansen, 2005). Sand et al. (2016) found that the surface temperature in the Arctic is most sensitive to emissions in Arctic countries, and Asian countries contribute greatly to Arctic warming because of the large absolute amount of emissions. With these large disagreements among studies, it is thus necessary to unveil BC sources in the Arctic with high precision simulations.

Various models have been used to investigate BC sources in the Arctic. Depending on the simulation method, these models are generally categorized as Lagrangian transport models (Hirdman et al., 2010; Liu et al., 2015; Stohl et al., 2006, 2013), chemical transport models (Ikeda et al., 2017; Koch and Hansen, 2005; Qi et al., 2017; Shindell et al., 2008; Wang et al., 2011; Xu et al., 2017), and global climate models (Ma et al., 2013; Schacht et al., 2019; H. Wang et al., 2014) (Table 1). The treatment of wet-scavenging parameterizations is a key factor affecting the model performance, which determines the uncertainties related to BC

89 particle removal (Kipling et al., 2013; Schacht et al., 2019; Q. Wang et al., 2014). The use of
90 emission inventories is another important factor that affects the simulation results (Dong et
91 al., 2019). The observations of BC that are used for model comparisons may be biased by
92 30 % depending on the method used (Sinha et al., 2017; Sharma et al., 2017). There are still
93 large uncertainties regarding the sources of BC in the Arctic with respect to emission sectors
94 (anthropogenic sources and open biomass burning) and geospatial contributions (Eckhardt
95 et al., 2015).

96 The FLEXible PARTicle dispersion model (Flexpart) had been used to investigate the
97 transport pathways and source contributions of BC in the Arctic (Stohl et al., 1998, 2006,
98 2013). Of Flexpart model up to version 9, wet removal was treated considering below-cloud
99 and within-cloud scavenging processes (Hertel et al., 1995; McMahon and Denison, 1979),
100 which depends on cloud liquid water content, precipitation rate and the depth of the cloud.
101 However, clouds were parameterized based on relative humidity, clouds frequently
102 extended to the surface and at times no clouds could be found in grid cells, with unrealistic
103 precipitation (Grythe et al., 2017). Recently, version 10 of Flexpart had been developed in
104 which cloud is differentiated into liquid, solid, and mixed phase, the cloud distribution is
105 more consistent with the precipitation data (Grythe et al., 2017). This improvement in the
106 cloud distribution and phase leads to a more realistic distribution of below-cloud and in-
107 cloud scavenging events. In this study, we quantified region-separated sources of BC in the
108 Arctic in 2010 by using Flexpart v10.1. We first evaluated the model performance by
109 comparing the results with those based on observations at surface sites. The source
110 contributions of emission sectors and geospatial contributions were evaluated by
111 incorporating the Arctic BC footprint into the emission inventories.

112 **2 Materials and methods**

113 2.1 Transport model

114 The Flexpart model (version 10.1) was run in backward mode to simulate BC footprints in
115 the Arctic region. The calculation of wet deposition was improved compared with those in
116 previous versions because in-cloud scavenging and below-cloud scavenging of particles were
117 separately calculated (Grythe et al., 2017). In previous versions of Flexpart, in the in-cloud
118 scavenging scheme, the aerosol scavenging coefficient depended on the cloud water
119 content, which was calculated according to an empirical relationship with precipitation rate,
120 in which all aerosols had the same nucleation efficiency (Hertel et al., 1995 ; Stohl et al.,
121 2005). In the new version, the in-cloud scavenging scheme depends on the cloud water
122 phase (liquid, ice, or mixed phase). Aerosols were set as ice nuclei for ice clouds and as
123 cloud condensation nuclei for liquid-water clouds, respectively. For mixed-phase clouds, it
124 was assumed that 10 % of aerosols are ice nuclei and 90 % are cloud condensation nuclei,
125 because BC is much more efficiently removed in liquid water clouds than in ice clouds (Cozic
126 et al., 2007; Grythe et al., 2017). The below-cloud scavenging scheme can parameterize
127 below-cloud removal as a function of aerosol particle size, and precipitation type (snow or
128 rain) and intensity. The biases produced in simulations using the new scheme are therefore
129 smaller than those in the old scheme for wet deposition of aerosols, especially at high
130 latitudes (Grythe et al., 2017).

131 The Arctic region is defined as areas north of 66° N. The potential BC emission
132 sensitivities at two heights in the Arctic region, i.e., the surface (0–500 m) and 5000 m
133 (4750–5250 m), were simulated. The Flexpart outputs were set as gridded retention times.
134 We performed tests at 500, 2000, and 5000 m, and chose 500 m as the upper boundary
135 height of the model output. The model was driven with operational analytical data from the
136 European Centre for Medium-Range Weather Forecasts (ECMWF) at a spatial resolution of

137 1° × 1° with 61 vertical levels. Temporally, ECMWF has a resolution of 3 h, with 6 h analysis
138 and 3 h forecast time steps. The simulation period was set at 60 days backward starting
139 from each month in 2010. The maximum life time of BC was set at 20 days because its
140 suspension time in the upper atmosphere during long-range transport is longer than that at
141 the surface level (Stohl et al., 2013). We implemented the wet deposition scheme in the
142 backward calculations, but it was not represented in the default setting (Flexpart v10.1,
143 https://www.flexpart.eu/downloads, obtained 10 April 2017).

144 The chemistry and microphysics could not be resolved by Flexpart. The model therefore
145 ignores hydrophobic to hydrophilic state changes and size changes of BC, and assumes that
146 all BC particles are aged hydrophilic particles. This may lead to an overestimation of BC
147 removal and hence force underestimation of simulated BC concentration, especially of fossil
148 fuel combustion sources where BC could be in the hydrophobic state for a few days. A
149 logarithmic size distribution of BC with a mean diameter of 0.16 μm and a standard
150 deviation of 1.96, in accordance with our ship observations in the Arctic, was used (Taketani
151 et al., 2016). The particle density was assumed to be 2000 kg m^{-3}, and 1 million
152 computational particles were randomly generated in the Arctic region for the backward
153 runs.

154 Four ground-based observations made during the period 2007–2011 were used to
155 validate the model performance. The potential BC emission sensitivity at 0–500 m above
156 ground level from a 0.1° grid centered at each site was simulated. Other model
157 parameterizations were consistent with those for the Arctic region, except that 200 000
158 computational particles were released.

159 2.2 Emission inventories

We focused on BC sources from anthropogenic emissions and open biomass burning. The Hemispheric Transport of Air Pollution version 2 inventory (HTAP2) for 2010 was used for monthly anthropogenic BC emissions (Janssens-Maenhout et al., 2015), which include sectors from energy, industry, residential and transport. It is worth noting that the residential sector includes not only combustions of fossil fuels, but also biofuels. However, as it has been reported that BC emissions in Russia were underestimated in HTAP2, we used the BC emissions reported by Huang et al. (2015) for Russia, in which the annual BC emissions were 224 Gg yr^{-1}. For open biomass burning, we used the monthly BC emissions from the Global Fire Emissions Database version 3 inventory (GFED3) (van der Werf et al., 2010) for the purposes of intercomparison with other studies, as this version is widely used. The term "open biomass burning" here indicates burning of biomass in the open field as is determined by the remote sensing measurement basis, including forest, agricultural waste, peat fires, grassland and savanna, woodland, deforestation and degradation, where biofuel burning for residential use is not included. Geospatial distributions of emissions from anthropogenic sources and open biomass burning in January and July are shown in Fig. S1.

2.3 Calculation of Arctic BC source contributions

The source contributions to Arctic BC were derived by incorporating the gridded retention time into the column emission flux, which was derived from the emission inventories in each grid. Calculations for anthropogenic sources and open biomass burning were performed separately and the sum was used. For anthropogenic sources, the regions were separated into North America and Canada (25–80° N, 50–170° W), Europe (30–80° N, 0–30° E), Russia (53–80° N, 30–180° E), East Asia (35–53° N, 75–150° E and 20–35° N, 100–150° E), and others (the rest) (Fig. 1a). For open biomass burning sources, the regions were

183 separated into Alaska and Canada (50–75° N, 50–170° W), Siberia (50–75° N, 60–180° E),
184 and others (Fig. 1b).

185 2.3 Observations

186 BC levels simulated by Flexpart were compared with those based on surface observations
187 at four sites: Barrow, USA (156.6° W, 71.3° N, 11 m asl), Alert, Canada (62.3° W, 82.5° N,
188 210 m asl), Zeppelin, Norway (11.9° E, 78.9° N, 478 m asl), and Tiksi, Russia (128.9° E, 71.6°
189 N, 8 m asl). Aerosol light absorption was determined by using particle soot absorption
190 photometers (PSAPs) at Barrow, Alert, and Zeppelin, and an aethalometer at Tiksi. For PSAP
191 measurements, the equivalent BC values were derived using a mass absorption efficiency of
192 10 m^2 g^{-1}. The equivalent BC at Tiksi, which was determined with an aethalometer, was
193 obtained directly. These measurement data were obtained from the European Monitoring
194 and Evaluation Programme and World Data Centre for Aerosols database
195 (http://ebas.nilu.no) (Tørseth et al., 2012).

196 It is worth noting that uncertainties could be introduced by using different BC
197 measurement techniques. An evaluation of three methods for measuring BC at Alert,
198 Canada indicated that an average of the refractory BC determined with a single-particle soot
199 photometer (SP2) and elemental carbon (EC) determined from filter samples give the best
200 estimate of BC mass (Sharma et al., 2017). Xu et al. (2017) reported that the equivalent BC
201 determined with a PSAP was close to the average of the values for refractory BC and EC at
202 Alert. In this study, we consider that the equivalent BC values determined with a PSAP at
203 Barrow, Alert, and Zeppelin to be the best estimate. There may be uncertainties in the
204 equivalent BC observations performed with an aethalometer at Tiksi because of co-existing
205 particles such as light-absorptive organic aerosols, scattering particles, and dusts
206 (Kirchstetter et al., 2004; Lack and Langridge, 2013). Interference by the filter and

uncertainties in the mass absorption cross section could also contribute to the bias observed in measurements made with an aethalometer at Tiksi.

3 Results and discussion

3.1. Comparisons of simulations with BC observations at Arctic surface sites

Flexpart generally reproduced the seasonal variations in BC at four Arctic sites well [Pearson correlation coefficient (R) = 0.53–0.80, root-mean-square error (RMSE) = 15.1–56.8 ng m^{-3}] (Fig. 2). Winter maxima were observed for the four sites, while a secondary elevation was observed for Alert and Tiksi. At Barrow, the observed high values of BC were unintentionally excluded during data screening in the forest fire season in summer (Stohl et al., 2013); the original observed BC is supposed to be higher as was reflected by the simulation. This seasonality is probably related to relatively stronger transport to the Arctic region in winter, accompanied by lower BC aging and inefficient removal, as simulated by older versions of Flexpart (Eckhardt et al., 2015; Stohl et al., 2013).

From January to May at Barrow and Alert, the mean BC simulated by Flexpart v10.1 were 32.2 ng m^{-3} and 31.2 ng m^{-3}, respectively. Which was 46 % lower than the observations (59.3 ng m^{-3} and 58.2 ng m^{-3}, respectively). This is probably related to the inadequate BC emission in the inventory, although seasonal variations in residential heating are included in HTAP2, which would reduce the simulation bias (Xu et al., 2017). Simulations by GEOS-Chem using the same emission inventories also underestimated BC levels at Barrow and Alert (Ikeda et al., 2017; Xu et al., 2017). The underestimation by Flexpart could also be partly contributed by the assumption that all particles are hydrophilic, where the BC scavenging could be overestimated. The corresponding uncertainties are larger in winter months, when there are more sources from fossil fuel combustion.

At Zeppelin, the Flexpart-simulated BC (39.1 ng m^{-3} for annual mean) was 85 % higher than the observed value (21.1 ng m^{-3} for annual mean), especially in winter (112% higher). It has been reported that riming in mixed-phase clouds occurs frequently at Zeppelin (Qi et al., 2017). During the riming process, BC particles act as ice particles and collide with the relatively numerous water drops, which form frozen cloud droplets, and then snow is precipitated. This results in relatively efficient BC scavenging (Hegg et al., 2011). Such a process could not be dealt with by the model. At Tiksi, Flexpart underestimated BC (74.4 ng m^{-3} for annual mean) in comparison with observation (104.2 ng m^{-3} for annual mean). Other than the hydrophilic BC assumption and underestimated BC emission in the simulation as the cases for Barrow and Alert, the observations at Tiksi by an aethalometer could containing light-absorbing particles other than BC, resulting in higher observed concentrations if compared with those obtained by SP2, EC and PSAP.

Anthropogenic emissions are the main sources of BC at the four Arctic sites from late autumn to spring, whereas open biomass burning emissions make large contributions in summer. From October to April, anthropogenic emissions accounted for 87–100 % of BC sources at all the observation sites. At Barrow, open biomass burning accounted for 35–78 % of BC in June–September (Fig. 2). There are large interannual variations in both observed and simulated BC (Fig. S2). In June–August 2010, the mean contributions of open biomass burning to BC were 6.3, 2.4, and 8.6 times those from anthropogenic sources at Alert, Zeppelin, and Tiksi, respectively. In this study, we focused on BC in the Arctic region in 2010.

3.2 Potential emission sensitivity of Arctic BC

The potential emission sensitivities (footprint) of Arctic BC showed different patterns with respect to altitude. The Arctic surface is sensitive to emissions at high latitudes (>60°

N). Air masses stayed for over 60 s in each of the 1° grids from the eastern part of northern Eurasia and the Arctic Ocean before being transported to the Arctic surface in the winter, represented by January (Fig. 3a). In comparison, during the summer, represented by July, BC at the Arctic surface was mainly affected by air masses that originated from the Arctic Ocean and the Norwegian Sea (Fig. 3b). These results imply that local BC emissions within the Arctic regions, although relatively weak compared with those from the mid-latitude regions, could strongly affect Arctic air pollution. Local BC emissions are important in the wintertime because the relatively stable boundary layer does not favor pollution dispersion. Recent increases in anthropogenic emissions in the Arctic region, which have been caused by the petroleum industry and development of the Northern Sea Route, are expected to cause deterioration of air quality in the Arctic. Socio-economic developments in the Arctic region would increase local BC emissions, and this will be a non-negligible issue in the future (Roiger et al., 2015; Schmale et al., 2018).

BC at high altitudes (~ 5000 m) in the Arctic is more sensitive to mid-latitude (30–60° N) emissions, especially in wintertime. In January, air masses hovered over the Bering Sea and the North Atlantic Ocean before arriving at the Arctic (Fig. 3c). A notable corridor at 30–50° N covering Eurasia and the United States was the sensitive region that affected BC at high altitudes in the Arctic in January. These results indicate that mid-latitude emissions, especially those with relatively large strengths from East Asia, East America, and Europe, could alter the atmospheric constituents at high altitudes in the Arctic. Central to east Siberia was the most sensitive region for BC at high altitudes in the Arctic in July (Fig. 3d). These results suggest that pollutants from frequent and extensive wildfires in Siberia in summer are readily transported to high altitudes in the Arctic. Boreal fires are expected to occur more frequently and over larger burning areas under future warming (Veira et al.,

278 2016), therefore the atmospheric constituents and climate in the Arctic could undergo more
279 rapid changes.

280 **3.3 Seasonal variations and sources of Arctic surface BC**

281 Arctic surface BC showed clear seasonal variations, with a primary peak in winter–spring
282 (December–March, 61.8–82.8 ng m^{-3}) and a secondary peak in summer (July, 52.7 ng m^{-3}).
283 BC levels were relatively low in May–June (21.8–23.1 ng m^{-3}) and September–November
284 (34.1–40.9 ng m^{-3}) (Fig. 4a). This seasonality agrees with observations and simulations at
285 Alert, Tiksi, and Barrow if consider the unintentional data exclusion (Stohl et al., 2013), and
286 previous studies targeting the whole Arctic (Ikeda et al., 2017; Xu et al., 2017). Compared
287 with the study reported by Stohl et al. (2013), the current work using the new scheme
288 produced smaller discrepancies between the simulated data and observations. Although the
289 simulation periods (monthly means for 2007–2011 in this study and for 2008–2010 in the
290 old scheme) and the anthropogenic emission inventories (HTAP2 in this study and ECLIPSE4
291 in the previous study) are different, the new scheme shows potential for better representing
292 BC transport and removal processes in the Arctic.

293 The annual mean Arctic BC at the surface was estimated to be 48.2 ng m^{-3}. From October
294 to April, anthropogenic sources accounted for 96–100 % of total BC at the Arctic surface.
295 Specifically, anthropogenic emissions from Russia accounted for 61–76 % of total BC in
296 October–May (56 % annually), and was the dominant sources of Arctic BC at the surface.
297 From an isentropic perspective, the meteorological conditions in winter favored the
298 transport of pollutants from northern Eurasia to the lower Arctic, along with diabatic cooling
299 and strong inversions (Klonecki et al., 2003). In comparison, open biomass burning from
300 boreal regions accounted for 56–85 % (75 % on average) of Arctic BC at the surface in
301 summer; open biomass burning emissions from North America and Canada accounted for

302 54 % of total Arctic surface BC in June, and those from Siberia accounted for 59–61 % in
303 July–August. Wildfires in the boreal forests in summer had a major effect on air quality in
304 the Arctic.

305 On an annual basis, anthropogenic sources and open biomass burning emissions
306 accounted for 82 % and 18 %, respectively, of total Arctic surface BC. In which, gas flaring
307 and residential burning (including burning of fossil fuels and biofuels) are accounting for
308 36 % (28–57 % in October–March) and 15 % (13–25 % in October–March), respectively (Fig.
309 5a-b). Our results support Stohl et al. (2013) that residential combustion emissions,
310 especially in winter are important sources of Arctic BC (Table 1). We estimated a
311 contribution of gas flaring to Arctic surface BC of 17.5 ng m^{-3} (36% of total). In comparison,
312 the value was estimated as 11.8 ng m^{-3} using an average Arctic surface BC of 28 ng m^{-3} and
313 a fraction from gas flaring of 42 % evaluated by earlier versions of Flexpart (Stohl et al.,
314 2013; Winiger et al., 2019). The different contribution could be partly attributed to the
315 difference in gas flaring emission inventory. BC emission from gas flaring in Russia by Huang
316 et al. (2015) was used in the current study, where total BC emission from gas flaring in
317 Russia in 2010 was ca. 81.1 kilotonne, which was larger than the estimate of ca. 64.9
318 kilotonne by GAINS inventory (Klimont et al., 2017) used by Stohl et al. (2013). Moreover,
319 Adopting ECLIPSEv5 inventory as was used by Winiger et al. (2019), we estimated that gas
320 flaring was contributing 14.4 ng m^{-3} to Arctic surface BC using Flexpart v10.1, a value 22 %
321 higher than those obtained using Flexpart v9. This difference could be attributed to the
322 improvement of the wet-scavenging scheme by Flexpart v10.1.

323 A recent study based on isotope observations at the Arctic sites and Flexpart v9.2
324 simulation suggested that open biomass burning, including open field burning and
325 residential biofuel burning, contributed 39 % of annual BC in 2011–2015 (Winiger et al.,

2019) (Table 1). In comparison, we estimated that residential burning and open biomass burning together account for 33 % of total Arctic surface BC. As the residential burning in our study includes burning of both biofuels and fossil fuels, our results indicated that biomass burning has a relatively smaller contribution. Other than the differences in BC removal treatment between different versions of the model, the contribution difference could also be attributed to the different emission inventories and years (2010 versus 2011-2015).

The geospatial contributions of anthropogenic sources and open biomass burning emissions can be further illustrated by taking January and July as examples. In January, high levels of anthropogenic emissions from Russia (contributing 64 % of Arctic surface BC), Europe (18 %), and East Asia (9 %) were identified (Fig. 6a). Specifically, Yamalo-Nenets Autonomous Okrug in Russia, which has the largest reserves of Russia's natural gas and oil (Filimonova et al., 2018), was the most notable emission hotspot, which suggests gas-flaring sources. The Komi Republic in Russia was also identified as a strong anthropogenic emitter contributing to Arctic surface BC. These gas-flaring industrial regions in Russia (58–69° N, 68–81°E) together contributed 33 % and 31 % of Arctic surface BC for January and the annual mean, respectively. Recently, Dong et al. (2019) evaluated BC emission inventories using GEOS-Chem and proposed that using the inventory compiled by Huang et al. (2015) for Russia, in which gas flaring accounted for 36 % of anthropogenic emissions, had no prominent impact on the simulation performance in Russia and the Arctic. They suggested that use of a new global inventory for BC emissions from natural gas flaring would improve the model performance (Huang and Fu, 2016). These results suggest that inclusion of BC emissions from gas flaring on the global scale is necessary for further BC simulations.

In Europe, a relatively high contribution of anthropogenic emissions to Arctic surface BC in January was made by Poland (50–55° N, 15–24° E, contributing 4 % of Arctic surface BC) because of relatively large emission fluxes in the region (Fig. S1a). Anthropogenic emissions from East China, especially those north of ~33° N (33–43° N, 109–126° E), contributed perceptibly (5 %) to Arctic surface BC.

In July, contributions from anthropogenic sources shrank to those from Yamalo-Nenets Autonomous Okrug and Komi Republic in Russia, and contributed a lower fraction (3 % of Arctic surface BC) (Fig. 6b). Few open biomass burning sources contributed in January (Fig. 6c), but contributions from open biomass burning to Arctic surface BC in July can be clearly seen, mainly from the far east of Russia, Canada, and Alaska (Fig. 6d). Open biomass burning emissions from Kazakhstan, southwest Russia, southern Siberia, and northeast China also contributed to Arctic surface BC, although at relatively low strengths (Fig. 5d and Fig. S1d). However, the contributions from open biomass burning could be higher, as the MODIS burned area, the basis of GFED emission inventories, was underestimated for northern Eurasia by 16 % (Zhu et al., 2017). Evangeliou et al. (2016) estimated a relatively high transport efficiency of BC from open biomass burning emissions to the Arctic, which led to a high contribution, i.e., 60 %, from such sources to BC deposition in the Arctic in 2010. A recent study suggested that open fires burned in western Greenland in summer (31 July to 21 August 2017) could potentially alter the Arctic air composition and foster glacier melting (Evangeliou et al., 2019). Although the footprint of Arctic surface BC showed a relatively weak sensitivity to areas such as forests and tundra, in the boreal regions, pollutants from boreal wildfires could have greater effects on the Arctic air composition in summer under future warming scenarios (Veira et al., 2016).

3.4 Sources of Arctic BC at high altitudes

373 Arctic BC levels at high altitudes (4750–4250 m) showed the highest levels in spring
374 (March–April, 40.5–53.9 ng m^{-3}), followed by those in late autumn to early winter
375 (November–January, 36.5–40.0 ng m^{-3}), and summer (July–August, 33.0–39.0 ng m^{-3}) (Fig.
376 4c). The annual mean Arctic BC at high altitudes was estimated to be 35.2 ng m^{-3}, which is
377 ca. 73 % of those at the surface. Such a vertical profile is in accordance with those based on
378 aircraft measurements over the High Canadian Arctic (Schulz et al., 2019). Similarly to the
379 case for the surface, anthropogenic sources dominated by residential sectors, transport,
380 industry and energy (excluding gas flaring), accounted for 94–100 % of Arctic BC at high
381 altitudes in October–May (Figs. 4c, 5c). East Asia accounted for 34–65 % of the total BC in
382 October–May (40 % annually). In comparison, using the Community Atmosphere Model
383 version 5 driven by the NASA Modern Era Retrospective-Analysis for Research and
384 Applications reanalysis data and the IPCC AR5 year 2000 BC emission inventory, H. Wang et
385 al. (2014) found that East Asia accounted for 23% of BC burden in the Arctic for 1995–2005.
386 In summer, open biomass burning in the boreal regions accounted for 40–72 % (57 % on
387 average) of Arctic BC at high altitudes, similar to the source contributions to Arctic surface
388 BC. Specifically, open biomass burning sources from Siberia accounted for 40–42 % of Arctic
389 BC at high altitudes in July–August. Annually, anthropogenic sources and open biomass
390 burning accounted for 83 % (in which residential sources accounted for 34%) and 17 %,
391 respectively, of total Arctic BC at high altitudes (Figs. 4d, 5d).
392 Further investigations of geospatial contributions to Arctic BC at high altitudes in January
393 and July provided more details regarding BC sources. In January, the main anthropogenic BC
394 source in East Asia covered a wide range in China (Fig. 7a). Not only east and northeast
395 China, but also southwest China (Sichuan and Guizhou provinces) were the major
396 anthropogenic sources of Arctic BC at high altitudes. In July, anthropogenic sources made a

relatively weak contribution to Arctic BC at high altitudes. The regions that were sources of open biomass burning contributions to Arctic BC at high altitudes were mainly the far east of Siberia, Kazakhstan, central Canada, and Alaska, i.e., similar to the sources of Arctic surface BC. Unlike Arctic surface BC, for which the dominant source regions are at high latitudes in both winter and summer, Arctic BC at high altitudes mainly originates from mid-latitude regions (Figs. 6 and 7). In terms of transport pathways, air masses could be uplifted at low-to-mid latitudes and transported to the Arctic (Stohl, 2006). Further investigations are needed to obtain more details of the transport processes.

3.5 Comparison of Flexpart and GEOS-Chem simulations of BC sources

Data for BC sources simulated with Flexpart were compared with those obtained with GEOS-Chem (Ikeda et al., 2017), which is an Eulerian atmospheric transport model, using the same emission inventories. The simulated seasonal variations in Arctic BC levels and source contributions obtained with Flexpart agreed well with those obtained with GEOS-Chem (Fig. S3). The annual mean BC levels at the Arctic surface obtained by Flexpart and GEOS-Chem simulations were 48 and 70 ng m^{-3}, respectively; the high-altitude values simulated by Flexpart and GEOS-Chem were 35 and 38 ng m^{-3}, respectively. The magnitude difference between the BC levels at the Arctic surface could be related to meteorology. ECMWF ERA-Interim data were used as the input for the Flexpart simulation, whereas the GEOS-Chem simulation was driven by assimilated meteorological data from the Goddard Earth Observation System (GEOS-5).

The treatments of the BC removal processes could also lead to different simulation results, depending on the model. In terms of BC loss processes, dry and wet depositions were the removal pathways, depending on the particle size and density, in Flexpart. The treatment of meteorology, especially cloud water and precipitation, would therefore affect

421 the uncertainties of the simulations. In Flexpart version 10.1, BC particles are separately
422 parameterized as ice nuclei for ice clouds, cloud condensation nuclei for liquid-water clouds,
423 and 90 % as cloud condensation nuclei for mixed-phase clouds. The separation of mixed-
424 phase clouds is realistic, as 77 % of in-cloud scavenging processes occurred in the mixed
425 phase over a 90 day period starting from December 2006 (Grythe et al., 2017).

426 In GEOS-Chem simulations, the BC aging was parameterized based on the number
427 concentration of OH radicals (Liu et al., 2011). The BC was assumed to be hydrophilic in
428 liquid clouds ($T \geq 258$ K) and hydrophobic when serving as ice nuclei in ice clouds ($T < 258$ K)
429 (Wang et al., 2011), with modifications because the scavenging rate of hydrophobic BC was
430 reduced to 5 % of water-soluble aerosols for liquid clouds (Bourgeois and Bey, 2011). Such a
431 treatment is expected to improve the simulation accuracy (Ikeda et al., 2017).

432 In Lagrangian models, the trajectories of particles are computed by following the
433 movement of air masses with no numerical diffusion, although some artificial numerical
434 errors could be generated from stochastic differential equations (Ramli and Esler, 2016). As
435 a result, long-range transport processes can be well simulated (Stohl, 2006; Stohl et al.,
436 2013). In comparison, Eulerian chemical transport models such as GEOS-Chem have the
437 advantage of simulating non-linear processes on the global scale, which enables treatment
438 of the BC aging processes (coating with soluble components) (Bey et al, 2001; Eastham et
439 al., 2018). However, with GEOS-Chem, the capture of intercontinental pollution plumes is
440 difficult because of numerical plume dissipation (Rastigejev et al., 2010). Nevertheless, the
441 agreement between the Flexpart and GEO-Chem simulations of BC source contributions
442 indicates improved reliability of evaluated source contributions to Arctic BC.

443 **4 Conclusions**

444 The source contributions to Arctic BC were investigated by using a Flexpart (version 10.1)
445 transport model that incorporated emission inventories. Flexpart-simulated BC data agreed
446 well with observations at Arctic sites, i.e., Barrow, Alert, Zeppelin, and Tiksi. The source
447 regions and source sectors of BC at the surface and high altitudes (~ 5000 m) over a wide
448 region in the Arctic north of 66° N were simulated. BC at the Arctic surface was sensitive to
449 local emissions and those from nearby Nordic countries (>60° N). These results emphasize
450 the role of anthropogenic emissions such as gas flaring and development of the Northern
451 Sea Route in affecting air quality and climate change in the Arctic. Anthropogenic emissions
452 in the northern regions of Russia were the main source (56 %) of Arctic surface BC annually.
453 In contrast, BC in the Arctic at high altitudes was sensitive to mid-latitude emissions (30–60°
454 N). Although they are geospatially far from the Arctic, anthropogenic emissions in East Asia
455 made a notable (40 %) contribution to BC in the Arctic at high altitudes annually. Open
456 biomass burning emissions, which were mainly from Siberia, Alaska, and Canada, were
457 important in summer, contributing 56–85 % of BC at the Arctic surface, and 40–72 % at
458 Arctic high altitudes. Future increases in wildfires as a result of global warming could
459 therefore increase the air pollution level during the Arctic summer. This study clarifies the
460 source regions and sectors of BC in the Arctic. This information is fundamental for
461 understanding and tackling air pollution and climate change in the region.
462
463 *Data Availability.* The data set for simulated footprint and BC source contributions is
464 available on request to the corresponding author.
465
466 *Author contributions.* CZ and YK designed the study. CZ, MT, and IP optimized the Flexpart
467 model. CZ performed Flexpart model simulations, conducted analyses, and wrote the

manuscript. KI and HT provided data for GEOS-Chem simulations and site observations. All authors made comments that improved the paper.

Competing interests. The authors declare that they have no conflict of interest.

Financial Support. This study was supported by the Environmental Research and Technology Development Fund (2-1505) of the Ministry of the Environment, Japan.

Acknowledgment. We acknowledge staffs from the following university and agencies for BC observational data: Barrow and Tiksi sites are operated by National Oceanic and Atmospheric Administration; Zeppelin site is operated by Stockholm University; and Alert site is operated by Environment and Climate Change Canada. We are grateful to two anonymous reviewers for the comments. We thank Helen McPherson, PhD, from Edanz Group (www.edanzediting.com/ac) for editing a draft of this manuscript.

References

AMAP Assessment 2015: Black carbon and ozone as Arctic climate forcers, Arctic Monitoring and Assessment Programme (AMAP), Oslo, Norway, 2015.

Bey, I., Jacob, D. J., Yantosca, R. M., Logan, J. A., Field, B. D., Fiore, A. M., Li, Q. B., Liu, H. G. Y., Mickley, L. J., and Schultz, M. G.: Global modeling of tropospheric chemistry with assimilated meteorology: Model description and evaluation, J Geophys Res-Atmos, 106, 23073-23095, doi:10.1029/2001jd000807, 2001.

Bourgeois, Q. and Bey, I.: Pollution transport efficiency toward the Arctic: sensitivity to aerosol scavenging and source regions, J. Geophys. Res., 116, D08213, doi:10.1029/2010JD015096, 2011.

Brock, C. A., Cozic, J., Bahreini, R., Froyd, K. D., Middlebrook, A. M., McComiskey, A., Brioude, J., Cooper, O. R., Stohl, A., Aikin, K. C., de Gouw, J. A., Fahey, D. W., Ferrare, R.

A., Gao, R. S., Gore, W., Holloway, J. S., Hubler, G., Jefferson, A., Lack, D. A., Lance, S., Moore, R. H., Murphy, D. M., Nenes, A., Novelli, P. C., Nowak, J. B., Ogren, J. A., Peischl, J., Pierce, R. B., Pilewskie, P., Quinn, P. K., Ryerson, T. B., Schmidt, K. S., Schwarz, J. P., Sodemann, H., Spackman, J. R., Stark, H., Thomson, D. S., Thornberry, T., Veres, P., Watts, L. A., Warneke, C., and Wollny, A. G.: Characteristics, sources, and transport of aerosols measured in spring 2008 during the aerosol, radiation, and cloud processes affecting Arctic Climate (ARCPAC) Project, Atmospheric Chemistry and Physics, 11, 2423-2453, doi:10.5194/acp-11-2423-2011, 2011.

Cohen, J., Screen, J. A., Furtado, J. C., Barlow, M., Whittleston, D., Coumou, D., Francis, J., Dethloff, K., Entekhabi, D., Overland, J., and Jones, J.: Recent Arctic amplification and extreme mid-latitude weather, Nature Geoscience, 7, 627-637, doi:10.1038/Ngeo2234, 2014.

Cozic, J., Verheggen, B., Mertes, S., Connolly, P., Bower, K., Petzold, A., Baltensperger, U., and Weingartner, E.: Scavenging of black carbon in mixed phase clouds at the high alpine site Jungfraujoch, Atmos. Chem. Phys., 7, 1797-1807, doi:10.5194/acp-7-1797-2007, 2007.

Dong, X., Zhu, Q., Fu, J. S., Huang, K., Tan, J., and Tipton, M.: Evaluating recent updated black carbon emissions and revisiting the direct radiative forcing in Arctic, Geophysical Research Letters, 46, 3560– 3570. doi:10.1029/2018GL081242, 2019.

Eastham, S. D., Long, M. S., Keller, C. A., Lundgren, E., Yantosca, R. M., Zhuang, J. W., Li, C., Lee, C. J., Yannetti, M., Auer, B. M., Clune, T. L., Kouatchou, J., Putman, W. M., Thompson, M. A., Trayanov, A. L., Molod, A. M., Martin, R. V., and Jacob, D. J.: GEOS-Chem High Performance (GCHP v11-02c): a next-generation implementation of the GEOS-Chem chemical transport model for massively parallel applications, Geosci Model Dev, 11, 2941-2953, doi:10.5194/gmd-11-2941-2018, 2018.

Eckhardt, S., Quennehen, B., Olivie, D. J. L., Berntsen, T. K., Cherian, R., Christensen, J. H., Collins, W., Crepinsek, S., Daskalakis, N., Flanner, M., Herber, A., Heyes, C., Hodnebrog, O., Huang, L., Kanakidou, M., Klimont, Z., Langner, J., Law, K. S., Lund, M. T., Mahmood, R., Massling, A., Myriokefalitakis, S., Nielsen, I. E., Nojgaard, J. K., Quaas, J., Quinn, P. K., Raut, J. C., Rumbold, S. T., Schulz, M., Sharma, S., Skeie, R. B., Skov, H., Uttal, T., von Salzen, K., and Stohl, A.: Current model capabilities for simulating black carbon and sulfate concentrations in the Arctic atmosphere: a multi-model evaluation using a

527 comprehensive measurement data set, Atmospheric Chemistry and Physics, 15, 9413-
528 9433, doi:10.5194/acp-15-9413-2015, 2015.
529 Evangeliou, N., Balkanski, Y., Hao, W. M., Petkov, A., Silverstein, R. P., Corley, R., Nordgren,
530 B. L., Urbanski, S. P., Eckhardt, S., Stohl, A., Tunved, P., Crepinsek, S., Jefferson, A.,
531 Sharma, S., Nojgaard, J. K., and Skov, H.: Wildfires in northern Eurasia affect the budget of
532 black carbon in the Arctic - a 12-year retrospective synopsis (2002-2013), Atmospheric
533 Chemistry and Physics, 16, 7587-7604, doi:10.5194/acp-16-7587-2016, 2016.
534 Evangeliou, N., Kylling, A., Eckhardt, S., Myroniuk, V., Stebel, K., Paugam, R., Zibtsev, S., and
535 Stohl, A.: Open fires in Greenland in summer 2017: transport, deposition and radiative
536 effects of BC, OC and BrC emissions, Atmospheric Chemistry and Physics, 19, 1393-1411,
537 doi:10.5194/acp-19-1393-2019, 2019.
538 Filimonova, I. V., Komarova, A. V., Eder, L. V., and Provornaya, I. V.: State instruments for the
539 development stimulation of Arctic resources regions, IOP Conference Series: Earth and
540 Environmental Science, 193, 012069, doi:10.1088/1755-1315/193/1/012069, 2018.
541 Garrett, T. J., Brattstrom, S., Sharma, S., Worthy, D. E. J., and Novelli, P.: The role of
542 scavenging in the seasonal transport of black carbon and sulfate to the Arctic,
543 Geophysical Research Letters, 38, L16805, doi:10.1029/2011gl048221, 2011.
544 Grythe, H., Kristiansen, N. I., Zwaaftink, C. D. G., Eckhardt, S., Strom, J., Tunved, P., Krejci, R.,
545 and Stohl, A.: A new aerosol wet removal scheme for the Lagrangian particle model
546 FLEXPART v10, Geosci Model Dev, 10, 1447-1466, doi:10.5194/gmd-10-1447-2017, 2017.
547 Hegg, D. A., Clarke, A. D., Doherty, S. J., and Ström, J.: Measurements of black carbon
548 aerosol washout ratio on Svalbard, Tellus B, 63, 891–900, doi:10.1111/j.1600-
549 0889.2011.00577.x, 2011.
550 Hertel, O., Christensen, J. Runge, E. H., Asman, W. A. H., Berkowicz, R., Hovmand, M. F., and
551 Hov, O.: Development and testing of a new variable scale air pollution model – ACDEP,
552 Atmos. Environ., 29, 1267–1290, 1995.
553 Hirdman, D., Burkhart, J. F., Sodemann, H., Eckhardt, S., Jefferson, A., Quinn, P. K., Sharma,
554 S., Strom, J., and Stohl, A.: Long-term trends of black carbon and sulphate aerosol in the
555 Arctic: changes in atmospheric transport and source region emissions, Atmospheric
556 Chemistry and Physics, 10, 9351-9368, doi:10.5194/acp-10-9351-2010, 2010.
557 Huang, K., and Fu, J. S.: A global gas flaring black carbon emission rate dataset from 1994 to
558 2012, Scientific Data, 3, 160104. doi:10.1038/sdata.2016.104, 2016.

559 Huang, K., Fu, J. S., Prikhodko, V. Y., Storey, J. M., Romanov, A., Hodson, E. L., Cresko, J.,
560 Morozova, I., Ignatieva, Y., and Cabaniss, J.: Russian anthropogenic black carbon:
561 Emission reconstruction and Arctic black carbon simulation, J Geophys Res-Atmos, 120,
562 11306-11333, doi:10.1002/2015jd023358, 2015.
563 Ikeda, K., Tanimoto, H., Sugita, T., Akiyoshi, H., Kanaya, Y., Zhu, C. M., and Taketani, F.:
564 Tagged tracer simulations of black carbon in the Arctic: transport, source contributions,
565 and budget, Atmospheric Chemistry and Physics, 17, 10515-10533, doi:10.5194/acp-17-
566 10515-2017, 2017.
567 Janssens-Maenhout, G., Crippa, M., Guizzardi, D., Dentener, F., Muntean, M., Pouliot, G.,
568 Keating, T., Zhang, Q., Kurokawa, J., Wankmüller, R., Denier van der Gon, H., Kuenen, J. J.
569 P., Klimont, Z., Frost, G., Darras, S., Koffi, B., and Li, M.: HTAP_v2.2: a mosaic of regional
570 and global emission grid maps for 2008 and 2010 to study hemispheric transport of air
571 pollution, Atmos. Chem. Phys., 15, 11411–11432, doi:10.5194/acp-15-11411-2015, 2015.
572 Keegan, K. M., Albert, M. R., McConnell, J. R., and Baker, I.: Climate change and forest fires
573 synergistically drive widespread melt events of the Greenland Ice Sheet, P Natl Acad Sci
574 USA, 111, 7964-7967, doi:10.1073/pnas.1405397111, 2014.
575 Kipling, Z., Stier, P., Schwarz, J. P., Perring, A. E., Spackman, J. R., Mann, G. W., Johnson, C.
576 E., and Telford, P. J.: Constraints on aerosol processes in climate models from vertically-
577 resolved aircraft observations of black carbon, Atmos. Chem. Phys., 13, 5969–5986,
578 doi:10.5194/acp-13-5969-2013, 2013.
579 Kirchstetter, T. W., Novakov, T., and Hobbs, P. V.: Evidence that the spectral dependence of
580 light absorption by aerosols is affected by organic carbon, J Geophys Res-Atmos, 109,
581 D21208, doi:10.1029/2004jd004999, 2004.
582 Klimont, Z., Kupiainen, K., Heyes, C., Purohit, P., Cofala, J., Rafaj, P., Borken-Kleefeld, J., and
583 Schöpp, W.: Global anthropogenic emissions of particulate matter including black carbon,
584 Atmos. Chem. Phys., 17, 8681–8723, doi:10.5194/acp-17- 8681-2017, 2017.
585 Klonecki, A., Hess, P., Emmons, L., Smith, L., Orlando, J., and Blake, D.: Seasonal changes in
586 the transport of pollutants into the Arctic troposphere-model study, J Geophys Res-
587 Atmos, 108, 8367, doi:10.1029/2002jd002199, 2003.
588 Koch, D., and Hansen, J.: Distant origins of Arctic black carbon: A Goddard Institute for Space
589 Studies ModelE experiment, J Geophys Res-Atmos, 110, D04204,
590 doi:10.1029/2004jd005296, 2005.

591 Koch, D., Schmidt, G. A., and Field, C. V.: Sulfur, sea salt, and radionuclide aerosols in GISS
592 ModelE, J. Geophys. Res., 111, D06206, doi:10.1029/2004jd005550, 2006.
593 Lack, D. A., and Langridge, J. M.: On the attribution of black and brown carbon light
594 absorption using the Angstrom exponent, Atmospheric Chemistry and Physics, 13,
595 10535–10543, doi:10.5194/acp-13-10535-2013, 2013.
596 Law, K. S., and Stohl, A.: Arctic air pollution: Origins and impacts, Science, 315, 1537–1540,
597 doi:10.1126/science.1137695, 2007.
598 Liu, J., Fan, S., Horowitz, L. W., and Levy II, H.: Evaluation of factors controlling long-range
599 transport of black carbon to the Arctic, J. Geophys. Res., 116, D00A14,
600 doi:10.1029/2010JD015145, 2011.
601 Liu, D., Quennehen, B., Darbyshire, E., Allan, J. D., Williams, P. I., Taylor, J. W., Bauguitte, S. J.
602 B., Flynn, M. J., Lowe, D., Gallagher, M. W., Bower, K. N., Choularton, T. W., and Coe, H.:
603 The importance of Asia as a source of black carbon to the European Arctic during
604 springtime 2013, Atmospheric Chemistry and Physics, 15, 11537–11555, doi:10.5194/acp-
605 15-11537-2015, 2015.
606 Ma, P.-L., Rasch, P. J., Wang, H., Zhang, K., Easter, R. C., Tilmes, S., Fast, J. D., Liu, X., Yoon, J.-
607 H., and Lamarque, J.-F.: The role of circulation features on black carbon transport into the
608 Arctic in the Community Atmosphere Model version 5 (CAM5), J. Geophys. Res.-Atmos.,
609 118, 4657–4669, doi:10.1002/jgrd.50411, 2013.
610 McMahon, T. A. and Denison, P. J.: Empirical atmospheric deposition parameters – a survey,
611 Atmos. Environ., 13, 571–585, doi:10.1016/0004-6981(79)90186-0, 1979.
612 Najafi, M. R., Zwiers, F. W., and Gillett, N. P.: Attribution of Arctic temperature change to
613 greenhouse-gas and aerosol influences, Nature Climate Change, 5, 246-249,
614 doi:10.1038/Nclimate2524, 2015.
615 Park, R. J., Jacob, D. J., Palmer, P. I., Clarke, A. D., Weber, R. J., Zondlo, M. A., Eisele, F. L.,
616 Bandy, A. R., Thornton, D. C., Sachse, G. W., and Bond, T. C.: Export efficiency of black
617 carbon aerosol in continental outflow: Global implications, J Geophys Res-Atmos, 110,
618 D11205, doi:10.1029/2004jd005432, 2005.
619 Qi, L., Li, Q. B., Henze, D. K., Tseng, H. L., and He, C. L.: Sources of springtime surface black
620 carbon in the Arctic: an adjoint analysis for April 2008, Atmospheric Chemistry and
621 Physics, 17, 9697–9716, doi:10.5194/acp-17-9697-2017, 2017.

622 Quinn, P. K., Bates, T. S., Baum, E., Doubleday, N., Fiore, A. M., Flanner, M., Fridlind, A.,
623 Garrett, T. J., Koch, D., Menon, S., Shindell, D., Stohl, A., and Warren, S. G.: Short-lived
624 pollutants in the Arctic: their climate impact and possible mitigation strategies,
625 Atmospheric Chemistry and Physics, 8, 1723–1735, doi:10.5194/acp-8-1723-2008, 2008.
626 Ramli, H. M. and Esler, J. G.: Quantitative evaluation of numerical integration schemes for
627 Lagrangian particle dispersion models, Geosci. Model Dev., 9, 2441–2457,
628 doi:10.5194/gmd-9-2441-2016, 2016.
629 Rastigejev, Y., Park, R., Brenner, M., and Jacob, D.: Resolving intercontinental pollution
630 plumes in global models of atmospheric transport, J. Geophys. Res., 115, D02302,
631 doi:10.1029/2009JD012568, 2010.
632 Roiger, A., Thomas, J. L., Schlager, H., Law, K. S., Kim, J., Schafler, A., Weinzierl, B.,
633 Dahloktter, F., Krisch, I., Marelle, L., Minikin, A., Raut, J. C., Reiter, A., Rose, M., Scheibe,
634 M., Stock, P., Baumann, R., Bouapar, I., Clerbaux, C., George, M., Onishi, I., and Flemming,
635 J.: Quantifying emerging local anthropogenic emissions in the Arctic region: The ACCESS
636 aircraft campaign experiment, B. Am. Meteorol. Soc., 96, 441–460, doi:10.1175/Bams-D-
637 13-00169.1, 2015.
638 Sand, M., Berntsen, T. K., von Salzen, K., Flanner, M. G., Langner, J., and Victor, D. G.:
639 Response of Arctic temperature to changes in emissions of short-lived climate forcers,
640 Nature Climate Change, 6, 286-289, doi:10.1038/Nclimate2880, 2016.
641 Schacht, J., Heinold, B., Quaas, J., Backman, J., Cherian, R., Ehrlich, A., Herber, A., Huang, W.
642 T. K., Kondo, Y., Massling, A., Sinha, P. R., Weinzierl, B., Zanatta, M., and Tegen, I.: The
643 importance of the representation of air pollution emissions for the modeled distribution
644 and radiative effects of black carbon in the Arctic, Atmos. Chem. Phys., 19, 11159–11183,
645 doi:10.5194/acp-19-11159-2019, 2019.
646 Schmale, J., Arnold, S. R., Law, K. S., Thorp, T., Anenberg, S., Simpson, W. R., Mao, J., and
647 Pratt, K. A.: Local Arctic Air Pollution: A Neglected but Serious Problem, Earths Future, 6,
648 1385–1412, doi:10.1029/2018ef000952, 2018.
649 Schulz, H., Zanatta, M., Bozem, H., Leaitch, W. R., Herber, A. B., Burkart, J., Willis, M. D.,
650 Kunkel, D., Hoor, P. M., Abbatt, J. P. D., and Gerdes, R.: High Arctic aircraft measurements
651 characterising black carbon vertical variability in spring and summer, Atmospheric
652 Chemistry and Physics, 19, 2361–2384, doi:10.5194/acp-19-2361-2019, 2019.

653 Sharma, S., Leaitch, W. R., Huang, L., Veber, D., Kolonjari, F., Zhang, W., Hanna, S. J.,
654 Bertram, A. K., and Ogren, J. A.: An evaluation of three methods for measuring black
655 carbon in Alert, Canada, Atmospheric Chemistry and Physics, 17, 15225–15243,
656 doi:10.5194/acp-17-15225-2017, 2017.
657 Shaw, G. E.: The arctic haze phenomenon, B Am Meteorol Soc, 76, 2403–2413, 1995.
658 Shen, Z. Y., Ming, Y., Horowitz, L. W., Ramaswamy, V., and Lin, M. Y.: On the seasonality of
659 Arctic black carbon, J. Climate, 30, 4429–4441, doi:10.1175/Jcli-D-16-0580.1, 2017.
660 Shindell, D. T., Chin, M., Dentener, F., Doherty, R. M., Faluvegi, G., Fiore, A. M., Hess, P.,
661 Koch, D. M., MacKenzie, I. A., Sanderson, M. G., Schultz, M. G., Schulz, M., Stevenson, D.
662 S., Teich, H., Textor, C., Wild, O., Bergmann, D. J., Bey, I., Bian, H., Cuvelier, C., Duncan, B.
663 N., Folberth, G., Horowitz, L. W., Jonson, J., Kaminski, J. W., Marmer, E., Park, R., Pringle,
664 K. J., Schroeder, S., Szopa, S., Takemura, T., Zeng, G., Keating, T. J., and Zuber, A.: A multi-
665 model assessment of pollution transport to the Arctic, Atmos. Chem. Phys., 8, 5353-5372,
666 doi:10.5194/acp-8-5353-2008, 2008.
667 Sinha, P. R., Kondo, Y., Koike, M., Ogren, J. A., Jefferson, A., Barrett, T. E., Sheesley, R. J.,
668 Ohata, S., Moteki, N., Coe, H., Liu, D., Irwin, M., Tunved, P., Quinn, P. K., and Zhao, Y.:
669 Evaluation of ground-based black carbon measurements by filter-based photometers at
670 two Arctic sites, J Geophys Res-Atmos, 122, 3544-3572, doi:10.1002/2016jd025843,
671 2017.
672 Stohl, A., Forster, C., Frank, A., Seibert, P., and Wotawa, G.: Technical note: The Lagrangian
673 particle dispersion model FLEXPART version 6.2, Atmos. Chem. Phys., 5, 2461–2474,
674 doi:10.5194/acp-5-2461-2005, 2005.
675 Stohl, A.: Characteristics of atmospheric transport into the Arctic troposphere, J Geophys
676 Res-Atmos, 111, D11306, doi:10.1029/2005jd006888, 2006.
677 Stohl, A., Hittenberger, M., and Wotawa, G.: Validation of the Lagrangian particle dispersion
678 model FLEXPART against large-scale tracer experiment data, Atmos Environ, 32, 4245-
679 4264, doi:10.1016/S1352-2310(98)00184-8, 1998.
680 Stohl, A., Klimont, Z., Eckhardt, S., Kupiainen, K., Shevchenko, V. P., Kopeikin, V. M., and
681 Novigatsky, A. N.: Black carbon in the Arctic: the underestimated role of gas flaring and
682 residential combustion emissions, Atmospheric Chemistry and Physics, 13, 8833-8855,
683 doi:10.5194/acp-13-8833-2013, 2013.

684 Taketani, F., Miyakawa, T., Takashima, H., Komazaki, Y., Pan, X., Kanaya, Y., and Inoue, J.:
685 Shipborne observations of atmospheric black carbon aerosol particles over the Arctic
686 Ocean, Bering Sea, and North Pacific Ocean during September 2014, J Geophys Res-
687 Atmos, 121, 1914-1921, doi:10.1002/2015jd023648, 2016.
688 Tietze, K., Riedi, J., Stohl, A., and Garrett, T. J.: Space-based evaluation of interactions
689 between aerosols and low-level Arctic clouds during the Spring and Summer of 2008,
690 Atmospheric Chemistry and Physics, 11, 3359-3373, doi:10.5194/acp-11-3359-2011,
691 2011.
692 Tilling, R. L., Ridout, A., Shepherd, A., and Wingham, D. J.: Increased Arctic sea ice volume
693 after anomalously low melting in 2013, Nature Geoscience, 8, 643-646,
694 doi:10.1038/Ngeo2489, 2015.
695 Tørseth, K., Aas, W., Breivik, K., Fjæraa, A. M., Fiebig, M., Hjellbrekke, A. G., Lund Myhre, C.,
696 Solberg, S., and Yttri, K. E.: Introduction to the European Monitoring and Evaluation
697 Programme (EMEP) and observed atmospheric composition change during 1972–2009,
698 Atmos. Chem. Phys., 12, 5447–5481, doi:10.5194/acp-12-5447-2012, 2012.
699 Trusel, L. D., Das, S. B., Osman, M. B., Evans, M. J., Smith, B., Fettweis, X., McConnell, J. R.,
700 Noel, B. P. Y., and van den Broeke, M. R.: Nonlinear rise in Greenland runoff in response
701 to post-industrial Arctic warming, Nature, 564, 104-108, doi:10.1038/s41586-018-0752-4,
702 2018.
703 van der Werf, G. R., Randerson, J. T., Giglio, L., Collatz, G. J., Mu, M., Kasibhatla, P. S.,
704 Morton, D. C., DeFries, R. S., Jin, Y., and van Leeuwen, T. T.: Global fire emissions and the
705 contribution of deforestation, savanna, forest, agricultural, and peat fires (1997–2009),
706 Atmospheric Chemistry and Physics, 10, 11707-11735, doi:10.5194/acp-10-11707-2010,
707 2010.
708 Veira, A., Lasslop, G., and Kloster, S.: Wildfires in a warmer climate: Emission fluxes,
709 emission heights, and black carbon concentrations in 2090-2099, J Geophys Res-Atmos,
710 121, 3195-3223, doi:10.1002/2015jd024142, 2016.
711 Wang, H., Rasch, P. J., Easter, R. C., Singh, B., Zhang, R., Ma, P. L., Qian, Y., and Beagley, N.:
712 Using an explicit emission tag- ging method in global modeling of source-receptor
713 relationships for black carbon in the Arctic: Variations, Sources and Trans- port pathways,
714 J. Geophys. Res.-Atmos., 119, 12888–12909, doi:10.1002/2014JD022297, 2014.

715 Wang, Q., Jacob, D. J., Fisher, J. A., Mao, J., Leibensperger, E. M., Carouge, C. C., Le Sager, P.,
716 Kondo, Y., Jimenez, J. L., Cubison, M. J., and Doherty, S. J.: Sources of carbonaceous
717 aerosols and deposited black carbon in the Arctic in winter-spring: implications for
718 radiative forcing, Atmos. Chem. Phys., 11, 12453– 12473, doi:10.5194/acp-11-12453-
719 2011, 2011.
720 Wang, Q., Jacob, D. J., Spackman, J. R., Perring, A. E., Schwarz, J. P., Moteki, N., Marais, E. A.,
721 Ge, C., Wang, J., and Barrett, S. R. H.: Global budget and radiative forcing of black carbon
722 aerosol: constraints from pole-to-pole (HIPPO) observations across the Pacific, J.
723 Geophys. Res. Atmos., 119, 195–206, doi:10.1002/2013JD020824, 2014.
724 Winiger, P., Andersson, A., Eckhardt, S., Stohl, A., and Gustafsson, O.: The sources of
725 atmospheric black carbon at a European gateway to the Arctic, Nat Commun, 7, 12776,
726 doi:10.1038/ncomms12776, 2016.
727 Winiger, P., Barrett, T. E., Sheesley, R. J., Huang, L., Sharma, S., Barrie, L. A., Yttri, K. E.,
728 Evangeliou, N., Eckhardt, S., Stohl, A., Klimont, Z., Heyes, C., Semiletov, I. P., Dudarev, O.
729 V., Charkin, A., Shakhova, N., Holmstrand, H., Andersson, A., and Gustafsson, O.: Source
730 apportionment of circum-Arctic atmospheric black carbon from isotopes and modeling,
731 Sci Adv, 5, eaau8052, doi:10.1126/sciadv.aau8052, 2019.
732 Xu, J. W., Martin, R. V., Morrow, A., Sharma, S., Huang, L., Leaitch, W. R., Burkart, J., Schulz,
733 H., Zanatta, M., Willis, M. D., Henze, D. K., Lee, C. J., Herber, A. B., and Abbatt, J. P. D.:
734 Source attribution of Arctic black carbon constrained by aircraft and surface
735 measurements, Atmospheric Chemistry and Physics, 17, 11971-11989, doi:10.5194/acp-
736 17-11971-2017, 2017.
737 Yu, K., Keller, C. A., Jacob, D. J., Molod, A. M., Eastham, S. D., and Long, M. S.: Errors and
738 improvements in the use of archived meteorological data for chemical transport
739 modeling: an analysis using GEOS-Chem v11-01 driven by GEOS-5 meteorology, Geosci
740 Model Dev, 11, 305-319, doi:10.5194/gmd-11-305-2018, 2018.
741 Zhu, C., Kobayashi, H., Kanaya, Y., and Saito, M.: Size-dependent validation of MODIS
742 MCD64A1 burned area over six vegetation types in boreal Eurasia: Large underestimation
743 in croplands, Scientific reports, *7*, 4181, doi:10.1038/s41598-017-03739-0, 2017.

Table 1. Comparison of BC source contributions in the Arctic surface

Model and versions	Model type	Wet-deposition	Grid resolution	Meteorology	Emissions	Domain/Sites	Year/season	Major source regions/sectors	Reference
Flexpart-WRF 6.2	Lagrangian	Stohl et al. (2005)	unspecified	WRF forcast	ECLIPSE, FINN	continental Norway and Svalbard	spring 2013	Asian anthropogenic	Liu et al. (2015)
Flexpart 6.2	Lagrangian	Stohl et al. (2005)	1° × 1°	ECMWF operational	Unspecified (BC sensitivities were calculated)	Alert, Barrow, Zeppelin	1989-2009	Northern Eurasia	Hirdman et al. (2010)
Flexpart 6.2	Lagrangian	Stohl et al. (2005)	1° × 1°	ECMWF operational	ECLIPSE4(GAINS), GFED3	Arctic (north of 66°N)	2008-2010	Flaring (42%), residential (>20%)	Stohl et al. (2013)
Flexpart 9.2	Lagrangian	Stohl et al. (2005)	1° × 1°	ECMWF operational	ECLIPSE5(GAINS), GFED4.1	Arctic (north of 66.7°N)	2011-2015	Residential and open burning (39%)	Winiger et al. (2019)
Flexpart 10.1	Lagrangian	Grythe et al. (2017)	1° × 1°	ECMWF operational	HTAP2, GFED3, Huang et al. (2015) for Russia flaring	Arctic (north of 66°N)	2010	Flaring (36%), open burning (18%), residential (15%), others (31%)	Current study
GEOS-Chem 9.02	CTM	Wang et al. (2011)	2° × 2.5°	GEOS-5	HTAP2, GFED3, Huang et al. (2015) for Russia flaring	Arctic (north of 66°N)	2007-2011	Russia (62%)	Ikeda et al. (2017)
GEOS-Chem	CTM	Wang et al. (2011)	2° × 2.5°	GEOS-5	Bond et al. (2004), Zhang et al. (2009), GFED3	Alert, Barrow, Zeppelin	April 2008	Asian anthropogenic (35–45%), Siberian biomass burning (46–64%)	Qi et al. (2017)
GEOS-Chem	CTM	Wang et al. (2011)	2° × 2.5°	GEOS-5	Bond et al. (2007), FLAMBE	North America Arctic	April 2008	Open fire (50%)	Wang et al. (2011)

GEOS-Chem10.01	CTM	Wang et al. (2011)	2° × 2.5°	GEOS-5	HTAP2, ECLIPSE5, GFED4	Alert, Barrow, Zeppelin, Arctic (north of 66.5°N)	2009-2011	N-Asian anthropogenic (40–45%) in winter-spring	Xu et al. (2017)
GISS ModelE	GCM	Koch et al. (2006)	4° × 5°	Internal	Bond et al. (2004), Cooke and Wilson (1996)	Arctic (north of ~60°N)	Annual general	South Asia	Koch and Hansen (2005)

744

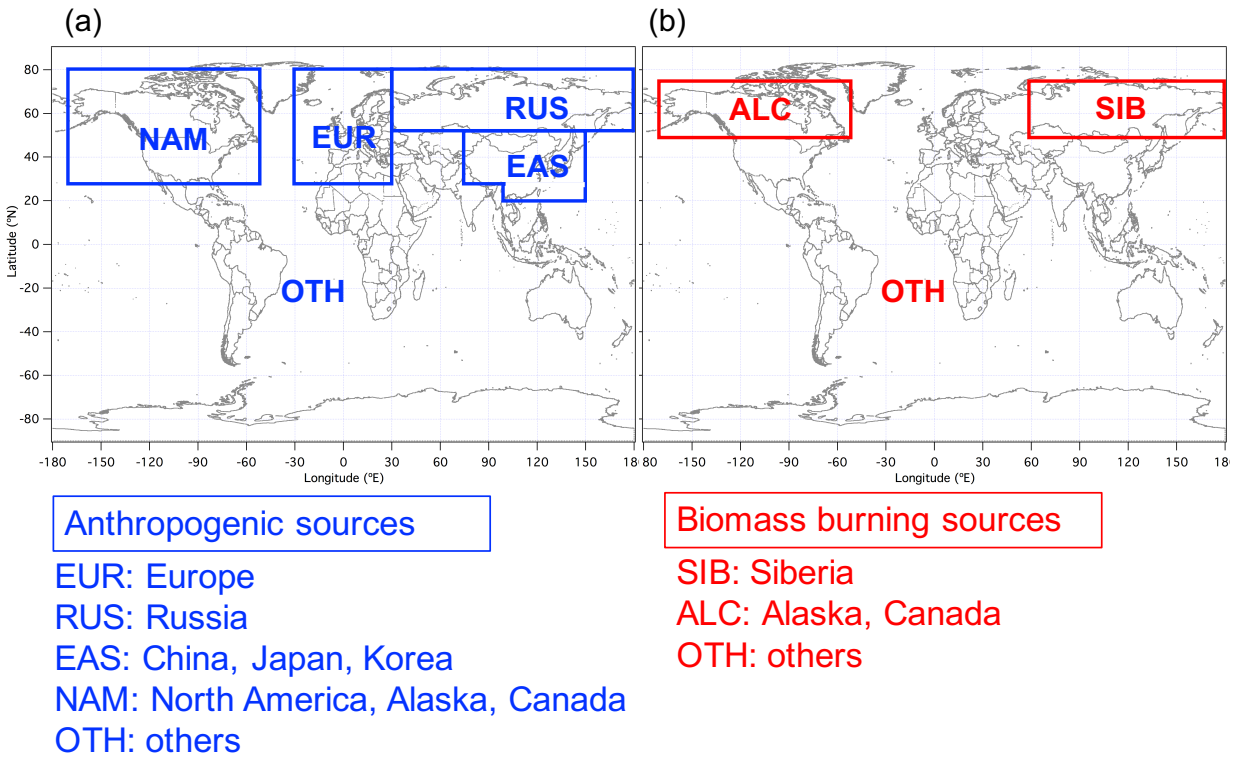

745

746 Figure 1. Regional separation for quantification of BC in the Arctic from (a) anthropogenic and

747 (b) open biomass burning sources.

748

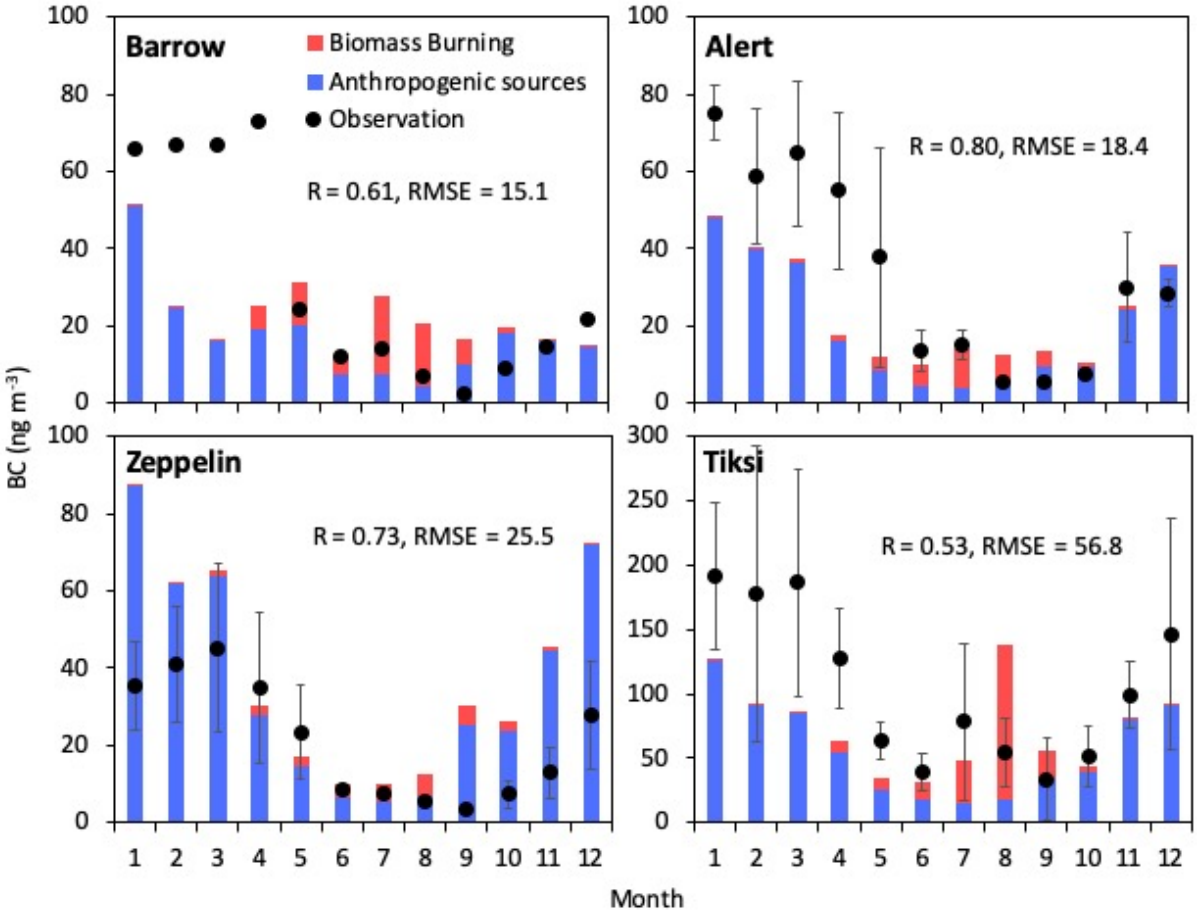

Figure 2. Observed (filled circles) and modeled (bars) seasonal variations in BC mass concentrations at Arctic sites. Contributions from anthropogenic sources (blue) and open biomass burning (red) in each month are shown. Monthly averages of observed (filled circles) and simulated (bars) BC were conducted for 2007–2011 at Alert, Canada (62.3° W, 82.5° N), and Zeppelin, Norway (11.9° E, 78.9° N), for 2009 at Barrow, USA (156.6° W, 71.3° N), and for 2010–2014 at Tiksi, Russia (128.9° E, 71.6° N). *R* and RMSE indicate correlation coefficient and root-mean-square error (ng m^{-3}), respectively.

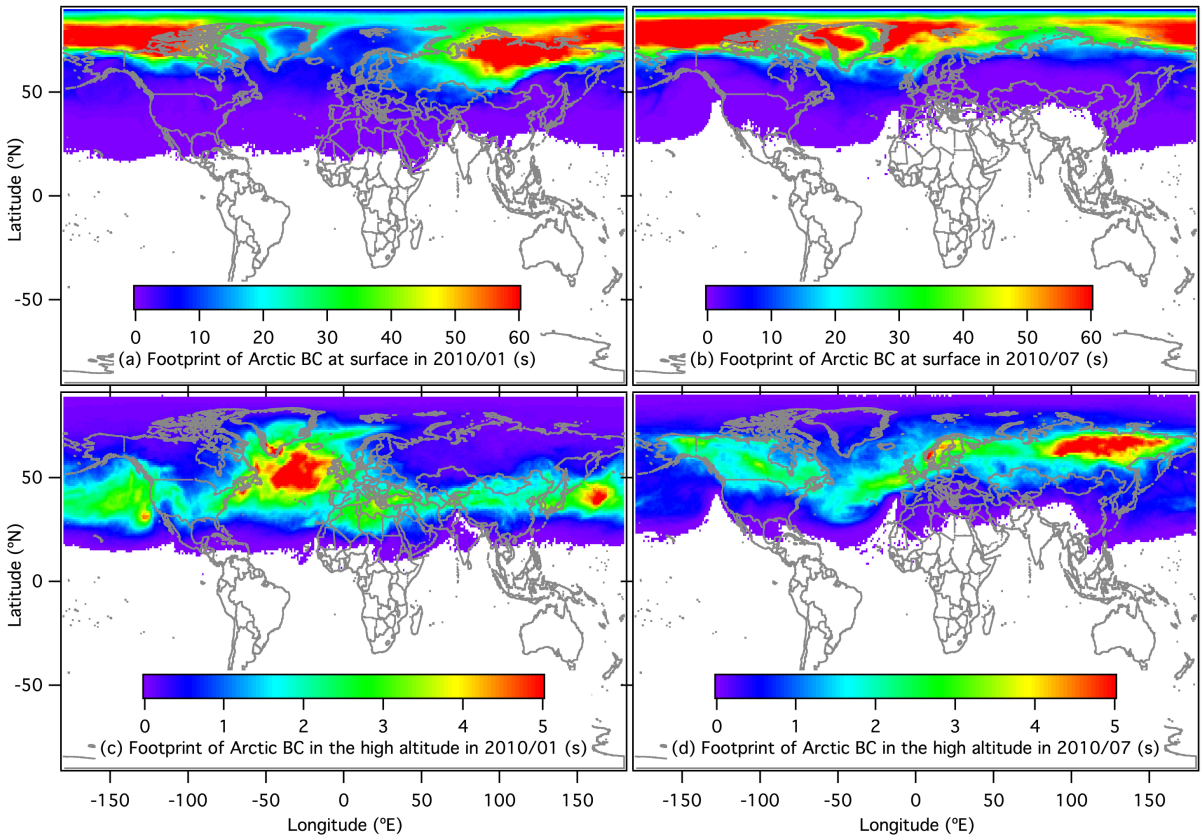

758

759 Figure 3. Footprints of Arctic BC shown as retention time(s) of (a) BC at surface (0–500 m) in
760 January 2010, (b) BC at surface in July 2010, (c) BC at high altitudes (4750–5250 m) in January
761 2010, and (d) BC at high altitudes (4750–5250 m) in July 2010.

762

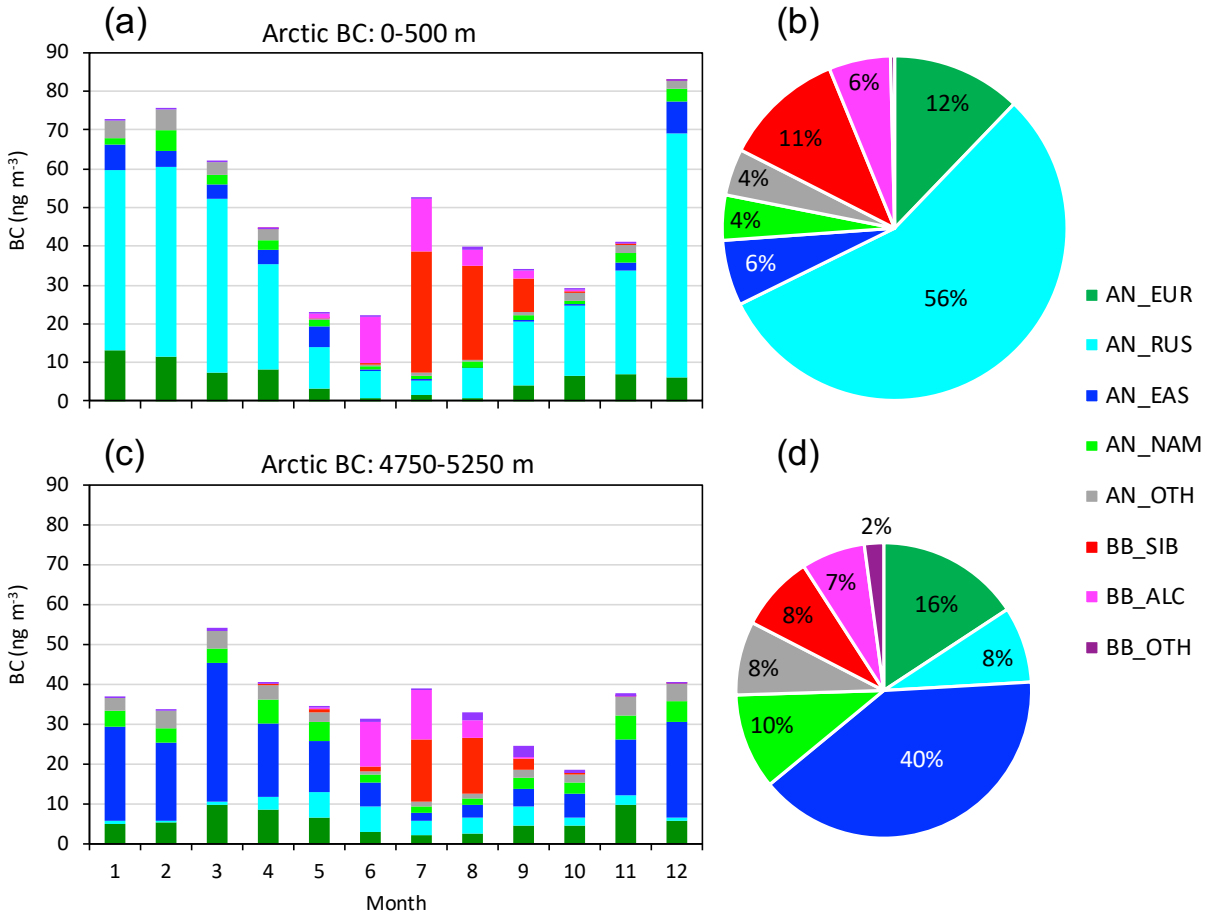

Figure 4. Contributions of anthropogenic sources and open biomass burning from each region to (a) seasonal variations in Arctic surface BC, (b) annual mean Arctic surface BC, (c) seasonal variations in Arctic BC at high altitudes, and (d) annual mean of Arctic BC at high altitudes.

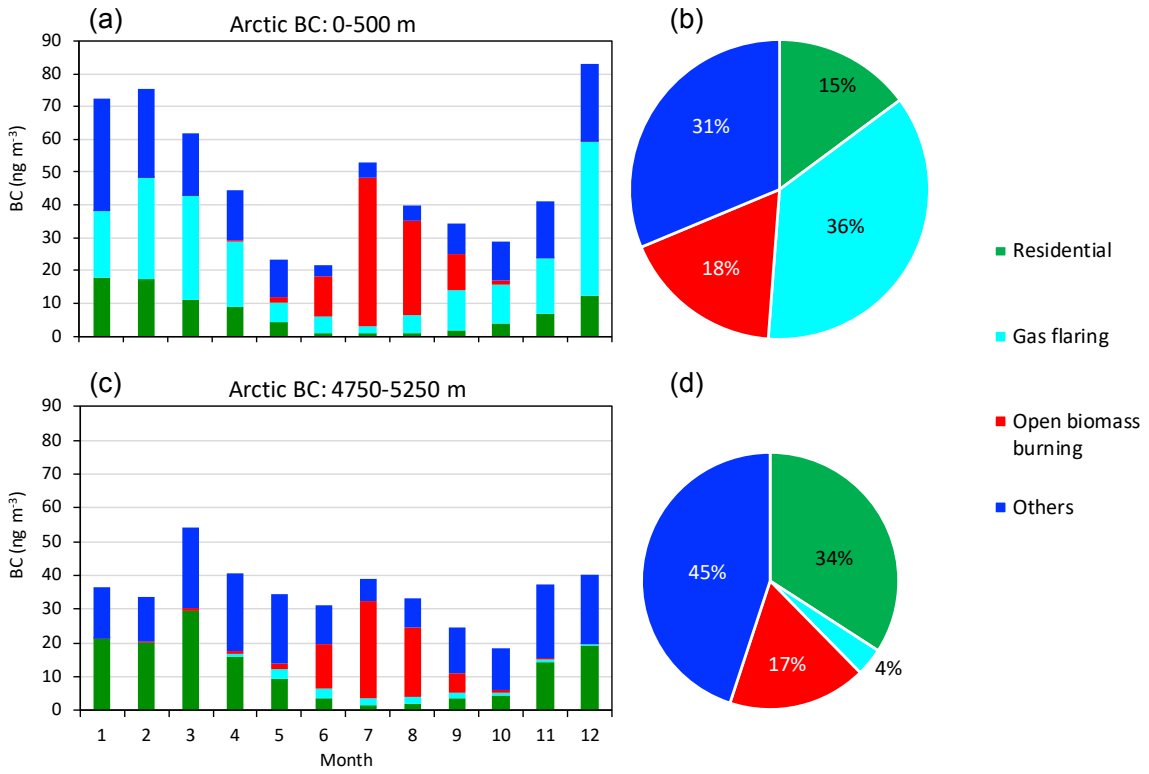

768

769 Figure 5. Sectorial contributions from residential combustion (including fossil fuel and biofuel
770 combustions), gas flaring, open biomass burning and others (energy other than gas flaring,
771 industry and transport) to (a) seasonal variations in Arctic surface BC, (b) annual mean Arctic
772 surface BC, (c) seasonal variations in Arctic BC at high altitudes, and (d) annual mean of Arctic
773 BC at high altitudes.

774

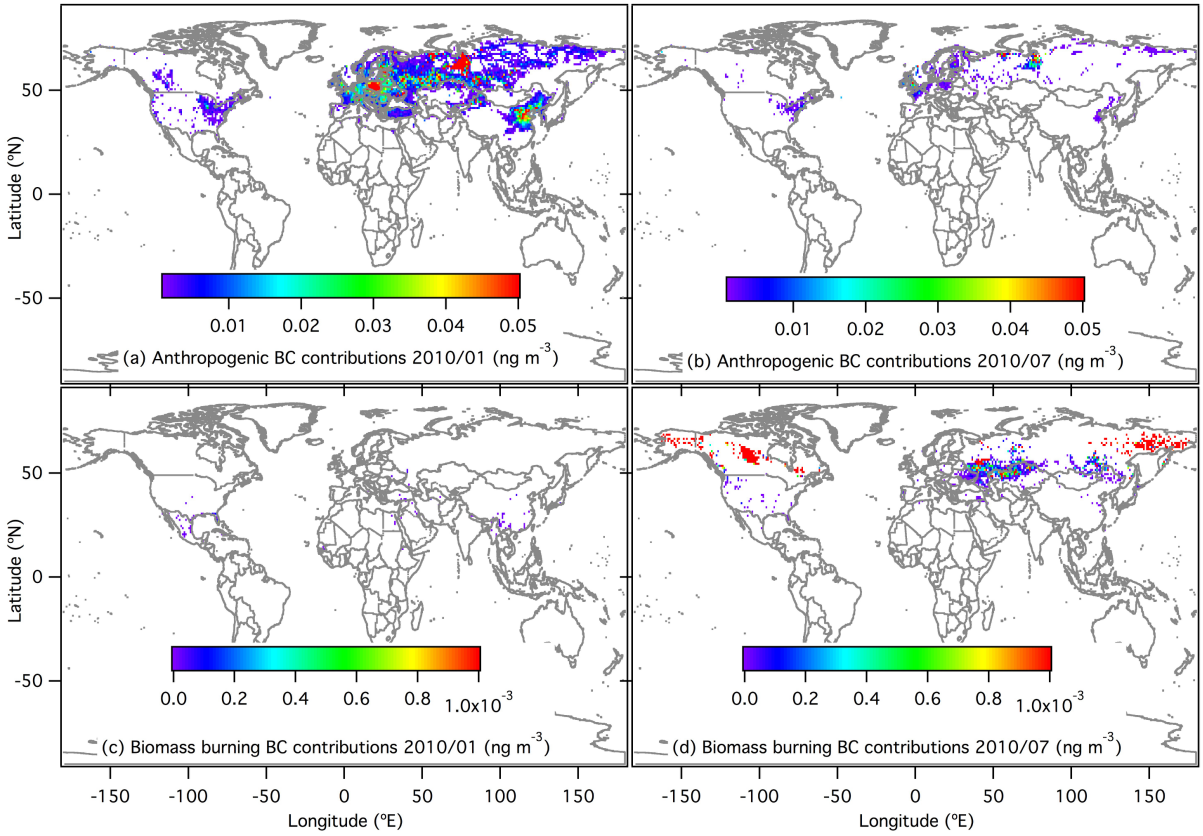

775

776 Figure 6. Spatial distributions of contributions to Arctic BC at surface (0–500 m) for (a)
777 anthropogenic contributions in January 2010, (b) anthropogenic contributions in July 2010, (c)
778 open biomass burning contributions in January 2010, and (d) open biomass burning
779 contributions in July 2010.

780

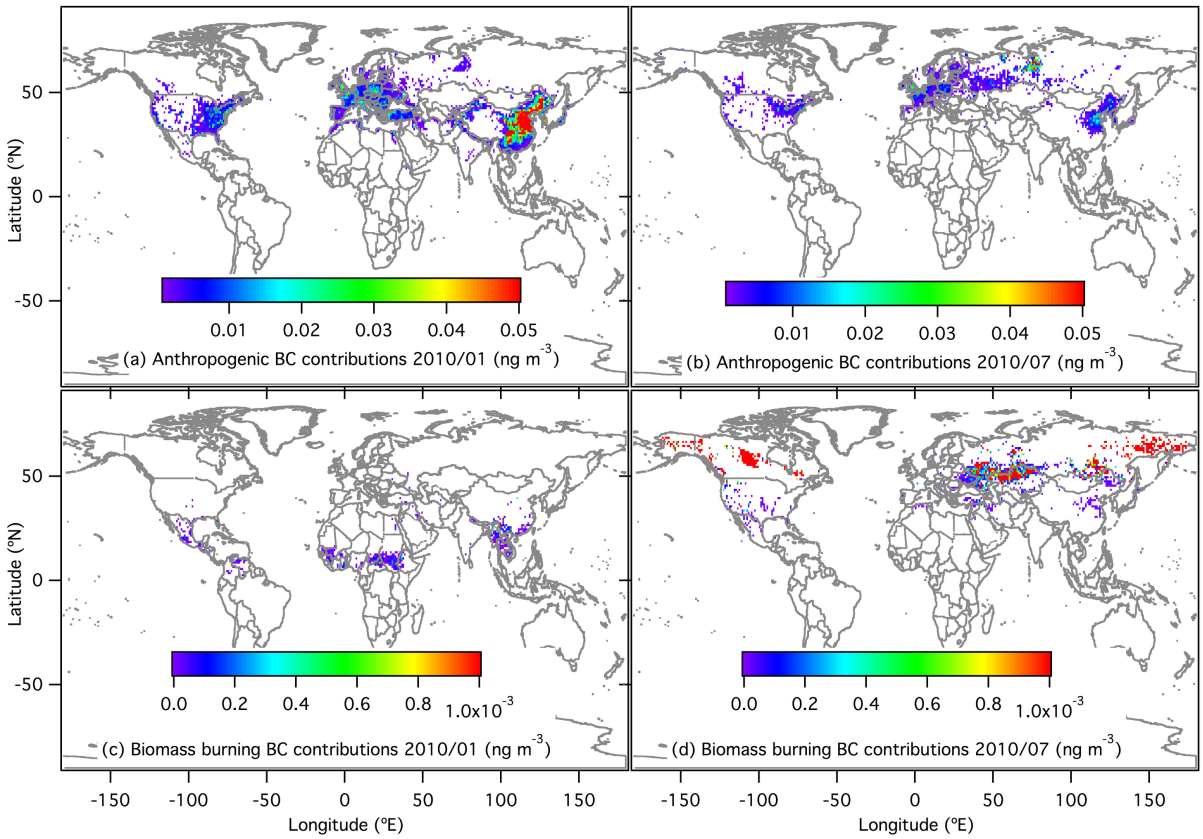

781

782 Figure 7. Spatial distributions of contributions to Arctic BC at high altitudes (4750–5250 m) for
783 (a) anthropogenic contributions in January 2010, (b) anthropogenic contributions in July 2010,
784 (c) open biomass burning contributions in January 2010, and (d) open biomass burning
785 contributions in July 2010.

786